Cancer Research

Re-engineering Vesicular Stomatitis Virus to Abrogate Neurotoxicity, Circumvent Humoral Immunity, and Enhance Oncolytic Potency

Alexander Muik[1], Lawton J. Stubbert[2], Roza Z. Jahedi[4], Yvonne Geiβ[1], Janine Kimpel[6], Catherine Dold[6], Reinhard Tober[6], Andreas Volk[1], Sabine Klein[2], Ursula Dietrich[1], Beta Yadollahi[3], Theresa Falls[2], Hrvoje Miletic[4,5], David Stojdl[3], John C. Bell[2], and Dorothee von Laer[6]

Abstract

As cancer treatment tools, oncolytic viruses (OV) have yet to realize what some see as their ultimate clinical potential. In this study, we have engineered a chimeric vesicular stomatitis virus (VSV) that is devoid of its natural neurotoxicity while retaining potent oncolytic activity. The envelope glycoprotein (G) of VSV was replaced with a variant glycoprotein of the lymphocytic choriomeningitis virus (LCMV-GP), creating a replicating therapeutic, rVSV (GP), that is benign in normal brain but can effectively eliminate brain cancer in multiple preclinical tumor models *in vivo*. Furthermore, it can be safely administered systemically to mice and displays greater potency against a spectrum of human cancer cell lines than current OV candidates. Remarkably, rVSV(GP) escapes humoral immunity, thus, for the first time, allowing repeated systemic OV application without loss of therapeutic efficacy. Taken together, rVSV(GP) offers a considerably improved OV platform that lacks several of the major drawbacks that have limited the clinical potential of this technology to date. *Cancer Res; 74(13); 3567–78. ©2014 AACR.*

Introduction

Despite extensive research, the prognosis for most nonhematologic cancers has not been significantly improved in the past two decades. This is especially true for cancers with disseminated metastases and for brain cancer (malignant gliomas), for which curative treatment is generally not available (1, 2). Oncolytic viruses (OV) offer the possibility to destroy malignant tissue while sparing normal cells. To date, clinical trials have proven this class of therapeutics to be safe, but usually lacking the potent antitumor activity necessary to clinically impact the disease (3, 4).

Vesicular stomatitis virus (VSV) is a particularly potent OV with impressive antitumor activity in preclinical models (5–11). Many aspects of VSV biology favor its development as an anticancer therapeutic. There is virtually no preexisting immunity in humans and the rare natural infections are generally asymptomatic. VSV shows no genetic reassortment, malignant transformation potential, or integration into the host genome (12). VSV infects a multitude of cancer cell types, where its highly cytopathic, rapid replication is independent of the cell cycle. The specificity for cancer cells is based on its high sensitivity to type I IFNs, whereby most cancers have a defective IFN system (reviewed in refs. 9 and 13). However, despite these preclinical accolades, development for human therapy, and especially as an intracranial agent has been hampered. Although wild-type VSV (wtVSV) has so far not been tested in humans, the strong neurotoxicity seen in rodents and nonhuman primates (14, 15) as well as the reported case of a VSV-induced encephalitis in a child (16), currently preclude the use of unattenuated VSV in doses required for an effective OV treatment.

To overcome this potential limitation, researchers have engineered neuroattenuated VSV with intracellular restrictions (miRNA-targeting) or modified tropism (transductional targeting; refs. 17 and 18). Whereas with miRNA-targeting strategies the reduced toxicity was shown to come at the expense of efficacy, exchanging the glycoprotein (i.e., pseudotyping) is expected to only interfere with host cell tropism. We and others recently described the use of heterologous envelope proteins, for example the glycoprotein of the nonneurotropic lymphocytic choriomeningitis virus WE54-strain (LCMV-GP) or single-chain variable antibody fragment (scFv)-modified measles virus glycoproteins, to either detarget VSV from neurons (LCMV-GP) or retarget VSV to cancer cells expressing discrete surface receptors (scFv-modified glycoproteins; refs. 19 and 20). However, in both cases replication-defective

Authors' Affiliations: [1]Georg-Speyer-Haus, Frankfurt am Main, Germany; [2]Ottawa Hospital Research Institute, Centre for Innovative Cancer Research; [3]Apoptosis Research Centre, Children's Hospital of Eastern Ontario, Ottawa, Ontario, Canada; [4]Department of Biomedicine, University of Bergen; [5]Department of Pathology, Haukeland University Hospital, Bergen, Norway; and [6]Institute for Virology, Innsbruck Medical University, Innsbruck, Austria

Note: Supplementary data for this article are available at Cancer Research Online (http://cancerres.aacrjournals.org/).

Current address for A. Muik: Medical Biotechnology and Gene Therapy, Paul-Ehrlich-Institut, Langen, Germany.

Corresponding Author: Dorothee von Laer, Innsbruck Medical University, Peter-Mayr-Straβe 4b, A-6020 Innsbruck, Austria. Phone: 43-512-900371700; Fax: 43-512-900373701; E-mail: dorothee.von-Laer@i-med.ac.at

doi: 10.1158/0008-5472.CAN-13-3306

viruses were pseudotyped in trans as a first proof-of-principle study.

Here, we sought to exploit the many virtues of replication-competent VSV as an anticancer therapeutic, while at the same time mitigating its neurotropism. We removed the VSV glycoprotein G, the key neurovirulence determinant (20–22), and replaced it with the arenavirus glycoprotein LCMV-GP (23–26), thereby generating rVSV(GP). While there are no doses at which wtVSV can be safely introduced into rodent brains, we found that rVSV(GP) caused no significant neurotoxicity even at doses of 10^8 plaque-forming units (PFU). In addition, rVSV (GP) was a much safer virus when delivered systemically compared with recombinant wtVSV (rVSV). rVSV(GP), however, retained rVSV's potent oncolytic activity in both syngeneic and xenogeneic orthotopic brain cancer models. Most importantly, in contrast to rVSV, rVSV(GP) was not inactivated by human serum complement and did not induce a neutralizing antibody (nAb) response in mice. The lack of nAb induction allowed rVSV(GP) to access and replicate within tumor tissue of preimmunized animals. Thus, rVSV(GP) is the first OV that has the potential to fully retain therapeutic efficacy upon repeated therapeutic application.

Materials and Methods

Cell lines

BHK-21, U87-MG, CT26 as well as the NCI60 cell panel were obtained from the American Type Culture Collection. G62 human glioblastoma cells were kindly provided by M. Westphal (University Hospital Eppendorf, Hamburg, Germany) and CT2A murine glioblastoma cells were a gift from T. Seyfried (Boston College, Chestnut Hill, MA; ref. 27). All cells were maintained in DMEM (Gibco) supplemented with 10% FBS and kept in a humidified atmosphere containing 5% CO_2 at 37°C. Cell lines were regularly tested for mycoplasma contamination and found to be negative.

Viruses

To exchange the *VSV-G* gene for *LCMV-GP* (LCMV-WE-HPI), the M-G intergenic region was amplified from pVSV-XN2 using the primers: 5′-CGATGAGCTCGATCAAGGTCAACCAGAGTATCACACTC-3′ and 5′-CAGTGGATCCGTGACGCGTAAACAGATCGATCTCTG-3′. The *LCMV-GP* sequence (GenBank accession no. AJ297484.1) was codon-optimized, synthesized *de novo* (GeneArt), and subcloned from pEFα-LCMV-GP into pBluescript-II (Stratagene) with *Eco*RI/*Sna*BI and *Eco*RI/*Hin*cII, respectively. The PCR product was digested with *Sac*I/*Bam*HI and cloned in front of the *LCMV-GP* gene. Finally, the *LCMV-GP* cassette was excised with *Mlu*I/*Xho*I and inserted into pVSV-XN2 and pVSV-GFP, replacing *VSV-G* to yield pVSV-GP and pVSV-GP-GFP, respectively (28). Recombinant viruses were rescued and plaque-purified as described previously (7). Titers were determined via plaque assay on confluent BHK-21 monolayers.

In vitro cytotoxicity assays

Cells were plated in 96-well plates at 10^4 cells/well. Spheroid formation was induced in 96-well plates precoated with 1% agar noble (Difco). Cell viability was assayed at the indicated time-points postinfection with rVSV and rVSV(GP) at MOI of 0.1 using the cell-proliferation agent WST-1 (Roche).

For determination of EC_{50}, 10^4 cells/well were seeded in 96-well plates and infected with rVSV, rVSVΔM51, or rVSV(GP) at MOIs of 0.0001-10. At 72 hours postinfection (hpi), viability was assayed by crystal violet staining (adherent cells) or Alamar Blue staining (AbD Serotec; suspension cells; HL60, K562, and Colo205). Wells with media alone were used as blank. The values were normalized against cells alone and EC_{50} values determined as the MOI at which 50% cytotoxicity was observed.

Mouse experiments general statement

All animal procedures were conducted with the approval of either the governmental board for the care of animal subjects (Regierungspräsidium Darmstadt, Germany) or the University of Ottawa Animal Care and Veterinary Service, Ottawa, Canada.

Neurotoxicity analysis

Indicated doses of rVSV/rVSV(GP)/rVSV(GP)-GFP were stereotactically injected in 6-week-old female Crl:CD1(ICR) mice (CD-1 mice; Charles River) as described previously (29). PBS-treated mice served as a surgical control. Animals were monitored for signs of neurologic disease (hind limb paralysis, ataxia) and weight changes to determine humane endpoints. In addition, 6- to 8-week-old female BALB/cAnNCrI mice (BALB/c mice; Charles River) were stereotactically injected with rVSV(GP)-GFP or rVSVΔM51-eGFP and monitored as described.

Immunohistochemistry

Animals were euthanized and transcardially perfused first with PBS, then 4% paraformaldehyde in PBS. Brains were removed and fixed in 4% paraformaldehyde. Coronal paraffin and/or cryo-sections were prepared. Paraffin sections were stained with either rabbit-anti-CD3 (Abcam; catalog no. ab5690), rabbit-anti-CD11b (Abcam; catalog no. ab75476) or rabbit-anti-cleaved caspase-3 (Cell Signaling; clone 5A1E) primary and biotinylated secondary antibody. Finally, sections were washed, incubated with ABC-complex (Vector Laboratories; catalog no. PK-7100) and treated with DAB (DAKO; catalog no. K3468). For quantification, 10 microscopic slides per individual stain were analyzed on a light microscope (Nikon) using Nikon imaging software.

Cryosections were stained with mouse-anti-NeuN (Millipore; clone A60) and mouse-anti-GFAP (Millipore; clone GA5) primary antibodies for neurons and astrocytes, respectively. Biotinylated goat-anti-mouse and goat-anti-rabbit (both Vector Laboratories; catalog no. BA-9200/BA-1000) were used as secondary antibodies. Sections were incubated with ExtrAvidin-Cy3 (Sigma; catalog no. E4142) and were analyzed by confocal scanning laser microscopy (Zeiss).

Systemic toxicity analysis

Six-week-old female CD-1 mice were injected intravenously (i.v.) with indicated doses of rVSV(GP) or rVSV in a total volume of 200 μL saline. PBS-treated mice served as negative

control. Animals were monitored and sacrificed when they showed neurologic signs suggesting neurotoxicity (hind–limb paralysis, ataxia) or if they lost $\geq$20% body weight. In addition, $n = 3$ CD1-mice/cohort were injected intravenously with either 10^8 PFU rVSV(GP), rVSV, or PBS. Blood samples were collected at indicated time-points. Serum alanine aminotransferase (ALT) levels were determined at the Central Laboratory of the Goethe University Hospital, Frankfurt. Creatinine levels were determined via the Creatinine Assay Kit (Abcam).

Biodistribution analysis

$N = 3$ 6-week-old female CD-1 mice per treatment group and time-point were injected intravenously with either PBS, 10^8 PFU rVSV(GP), or rVSV in a total volume of 200 μL. At the indicated time-points, blood was drawn and the respective cohorts were sacrificed and transcardially perfused with PBS. Organs were prepared and stored in RNAlater solution (Qiagen). RNA from blood and organs was purified using the QIAamp RNA blood and RNeasy Kit, respectively (Qiagen). RNA was reverse transcribed using the High Capacity RNA-to-cDNA Kit (Applied Biosystems) and VSV genomic RNA (gRNA) amounts were determined via real-time PCR ($n = 2$ replicates) using the VSV-specific NPqPCR primer set (29) as well as a PGK1 primer set for internal reference (PGK1f: 5′-TGACTTTGGACAAGCTGGACGTGA-3′; PGK1r: 5′-TTGATGCTTGGAACAGCAGCCTTG-3′; PGK1probe: 5′-LC610-TCGTGATGAGGGTGGACTTCAACGTT-BHQ2-3′). Real-time PCR was carried out with the TaqMan Gene Expression Master Mix (Applied Biosystems) using a LightCycler 480 Real-Time PCR System (Roche).

Subcutaneous tumor model

Six-week-old female NOD.CB17-*Prkdc*^{scid}/J mice (SCID mice; Jackson Laboratories) were inoculated subcutaneously with 10^6 G62 human glioblastoma cells as described previously (29). Once the tumors reached a volume of 0.1 cm^3, mice were treated intratumorally (i.t.) with two doses of 2×10^5 PFU rVSV (GP)-GFP, rVSV-GFP, or PBS as negative control. Bilateral tumors were treated alike. Mice were sacrificed when tumor volume exceeded 0.8 cm^3 or when they showed neurologic signs suggesting neurotoxicity.

In addition, $n = 2$ mice were sacrificed at 3 dpi and tumors were prepared. Tumors were fixed in 4% paraformaldehyde and sections (40 μm) were prepared on a VT1000S vibratome (Leica). Nuclear counterstaining was performed with TO-PRO-3 iodide (Invitrogen). Sections were analyzed by confocal laser scanning microscopy (Zeiss).

Intracranial tumor models

Six-week-old female SCID mice were stereotactically injected with 3×10^5 U87-RFP human glioma cells as described previously (8). At 10 days posttransplantation (dpt), the single-dose cohort was injected intravenously with 10^8 PFU rVSV (GP)-GFP in 200 μL PBS or pure PBS as control. Multidose-treated animals received two additional injections at 17 and 24 dpt. In addition, $n = 2$ U87-RFP tumor-bearing mice were treated intravenously with a single dose of 10^8 PFU rVSV(GP)-GFP at 10 dpt and sacrificed at 3 dpi. Brain sections (40 μm) were prepared on a VT1000S vibratome (Leica), counterstained with TO-PRO-3 iodide (Invitrogen), and analyzed by confocal laser scanning microscopy.

Six- to 8-week-old female C57Bl/6NCrl mice (C57Bl/6 mice; Charles River) were injected intracranially with 5×10^4 CT2A murine glioma cells as described above. At 7 dpt, mice were treated intratumorally with either 10 μL PBS or 10^8 PFU rVSV (GP)-GFP in PBS.

Six- to 8-week-old female Balb/C mice were injected intracranially with 3×10^4 CT26-lacZ cells as described above. One week after tumor implantation, mice were treated intratumorally with either 10 μL PBS or 2.5×10^7 PFU rVSV(GP)-GFP in PBS.

All animals were monitored for signs of neurologic disease and weight changes. Mice were sacrificed when they showed neurologic signs suggesting massive intracranial tumor load (circulation, ataxia) or if they lost $\geq$20% body weight.

Analysis of the nAb response and its effect on tumor delivery

Serum was prepared from 6- to 8-week-old female Balb/c mice on day 0. Subsequently, animals were immunized intravenously with 10^7 PFU of either rVSVΔM51 or rVSV (GP)-GFP. Mice were bled on day 3, 7, 14, and 21. Sera were prepared and nAb titers were determined as previously described (30).

In a separate experiment, at 10 dpi, immunized mice and unimmunized controls were grafted with 3×10^5 CT26-lacZ cells subcutaneously. When the average size of tumors reached approximately 0.25 cm^3, animals were treated with 10^8 PFU i.v. or 10^7 PFU i.t. of either rVSVΔM51 or rVSV(GP)-GFP. Immunized animals were treated with the respective virus used for preimmunization. At 48 hours posttreatment, mice were sacrificed and tumors were removed and stored in RNAlater solution. RNA was prepared using the RNeasy Kit and VSV gRNA levels in tumor tissue were determined by quantitative reverse transcriptase PCR (RT-PCR) using the StepOnePlus Real-Time PCR system (Invitrogen) in combination with the VSV-specific NPqPCR primer set (29). gRNA levels were calculated by means of a pVSV-XN2 standard curve.

Normal human serum inactivation studies

10^5 PFU of either rVSV or rVSV(GP) in 50 μL DMEM was mixed with 50 μL DMEM, 50 μL normal human serum (NHS) or 50 μL heat-inactivated NHS. Heat inactivation was performed as described elsewhere (31). The mixed samples were incubated for 45 minutes at 37°C and subsequently put on ice. Virus titers were determined via plaque assay on BHK-21 cells.

Statistical analysis

For comparison of measurements/sample groups with interval or ratio variables, statistical significance was determined using parametric, unpaired 2-tailed t test. Mouse survival curves were plotted as Kaplan–Meier analysis and statistical significance was determined using the log-rank test. $P < 0.05$ was regarded significant.

Results

Chimeric LCMV:VSV viruses lack neurotoxicity

To eliminate the neurotoxicity of wtVSV (herein referred to as rVSV, the recombinant virus generated from wtVSV cDNA sequence), we exchanged the glycoprotein (G), by the heterologous LCMV-WE-HPI envelope protein (GP). Novel, G-less viruses that expressed LCMV-GP [rVSV(GP)] were rescued and found to have similar growth kinetics to rVSV, although with somewhat reduced maximum titers (Supplementary Fig. S1). To directly evaluate neurotoxicity, escalating doses of rVSV (GP), rVSV, or the attenuated matrix protein-mutated rVSVΔM51 virus were injected into the brains of CD-1 and Balb/c mice. Consistent with previous reports (21, 22), all cohorts treated with VSV-G–expressing strains (doses as low as 10^1 PFU) succumbed to neurologic symptoms including significant weight loss by 9 days postinfection (dpi) (Fig. 1A–C). In contrast, all rVSV(GP)–treated CD-1 and Balb/c mice survived until the end of the 40 to 100 day observation period without any adverse effects, even when injected with doses up to 10^8 PFU. A smaller cohort of randomly selected CD-1 mice ($n = 5$) treated with 10^7 PFU rVSV(GP) were monitored for up to 250 days postinfection (dpi) with no signs of neurotoxicity (Fig. 1A).

We carried out histopathologic analysis of virus-injected animals to examine the extent of virus growth in mouse brain. Consistent with previous reports (14), confocal analysis of mouse brains at 3 dpi with 10^1 PFU rVSV-GFP revealed ongoing and extensive viral dissemination with multiple replicative foci of $NeuN^+/GFP^+$-infected neurons detectable throughout both hemispheres (Fig. 1D). As expected, these foci were associated with clear signs of encephalitis with significant numbers of inflammatory cells including perivascular $CD3^+$ lymphocytic infiltrates, activated $CD11b^+$ microglia, and apoptotic cells compared with PBS-treated controls (Supplementary Fig. S2; $P < 0.001$). In contrast, at 3 dpi rVSV (GP)-GFP–injected brains did not show any GFP-positive cells at any of the doses tested and only minimal needle track–associated reactive changes localized to the injection site.

rVSV(GP) is a safe systemic therapeutic

While substituting LCMV-GP for VSV-G strongly restricts VSV entry into normal cells of the central nervous system (CNS), we sought to determine if the chimeric virus had acquired new and unanticipated toxicities when administered systemically. CD-1 mice were intravenously injected with escalating doses ranging up to 10^9 PFU rVSV(GP) and compared and contrasted with rVSV treated animals. All virus treated animals showed significant weight loss between day 1

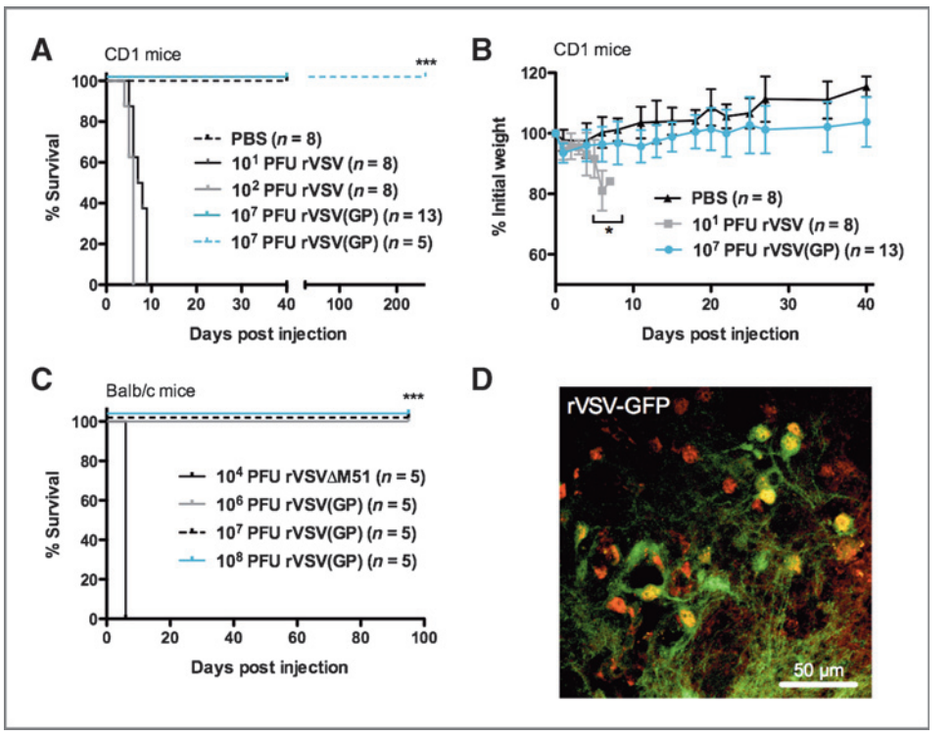

Figure 1. Intracerebral administration of high-dose rVSV(GP) does not result in neurotoxicity. Escalating doses of up to 10^8 PFU rVSV(GP) and decreasing doses as low as 10 PFU rVSV or 10^4 PFU rVSVΔM51 were injected into the right frontal lobe of CD-1 or Balb/c mouse brains ($n \geq 5$/cohort). PBS-treated mice served as negative control. Animals were monitored for signs of neurologic disease and were sacrificed when moribund. A, survival analysis of CD-1 mice for more than a period of 40 days. $N = 5$ randomly selected rVSV(GP)-treated mice were monitored up to 250 days. B, weight analysis of the respective CD-1 mice postinjection. Data points represent means ± SDs of each cohort at the respective time-point. C, as in A, but using Balb/c mice comparing rVSV(GP)-GFP to rVSVΔM51-eGFP. D, immunohistochemistry of rVSV-GFP–treated brains at 3 dpi. Neurons were counterstained with mouse anti-NeuN (clone A60) primary and Alexa Fluor 568–conjugated secondary antibody (red); *, $P < 0.05$; ***, $P < 0.001$.

and 3 postinjection when compared with PBS-treated controls (Fig. 2A and B, $P < 0.05$), however, even at the highest doses of rVSV(GP), treated animals rapidly regained weight and remained healthy. In contrast, rVSV-treated animals fared much worse with 2 of 6 mice having to be sacrificed because of neurotoxicity by day 4 when treated systemically at a dose of 1.58×10^8 PFU and 4 of 6 at 5×10^8 PFU i.v. (Fig. 2A).

To provide a more detailed analysis of potential off-target toxicity, sublethal doses of rVSV(GP) or rVSV were injected intravenously and serum ALT, creatinine as well as virus biodistribution kinetics were determined. Significant but mildly elevated ALT levels, suggestive of transient marginal hepatotoxicity, coincided with weight loss for both VSV-treated cohorts at days 1 and 2 postinjection with levels rapidly returning to baseline at day 3 (Fig. 2C, $P < 0.05$). ALT kinetics were virtually identical for rVSV(GP) and rVSV-injected animals. Creatinine levels were not elevated in any of the cohorts throughout the observation period, indicating a lack of renal toxicity (Fig. 2D).

In separate animal cohorts, quantitative RT-PCR was used to measure the distribution of viral genomes (gRNA) in treated animals over time in blood, brain, heart, kidney, liver, lung, and spleen. The biodistribution and kinetics of gRNA clearance for both rVSV and rVSV(GP) were indistinguishable in all of the major organs with the exception of the brain (Fig. 2E and Supplementary Fig. S3). rVSV established a productive but transient infection in the CNS with viral gRNA peaking at 3 dpi, whereas rVSV(GP) was rapidly cleared from the brains of treated animals and was already below detection limit at the time rVSV peaked (Fig. 2E, $P < 0.01$). For all the other tissues tested, both rVSV and rVSV(GP) were rapidly cleared with the exception of the spleen where viral gRNA persisted for at least 40 dpi (Supplementary Fig. S3), consistent with earlier reports (32).

rVSV(GP) is a potent oncolytic *in vitro*

Although rVSV(GP) is clearly a much safer virus compared with its parental rVSV strain, it was important to determine if this chimeric virus retained potent oncolytic activity. We determined the EC_{50} for rVSV, rVSVΔM51, and rVSV(GP) on the NCI-60 tumor cell panel and discovered that in general rVSV(GP) performed well and in many cell lines, including CNS malignancies, seemed more potent than the prototypical oncolytic rhabdovirus rVSVΔM51 (Fig. 3A). When tested against two human glioma cell lines, G62 and U87, rVSV(GP) performed on par with rVSV whether cells were cultured as monolayers (Supplementary Fig. S4) or spheroids (Fig. 3B). Both cell lines supported rapid replication (Supplementary Fig. S5), eventually leading to cell lysis within a few days.

rVSV(GP) is a potent oncolytic in *in vivo* preclinical models

Initially, G62 human glioma cells were engrafted subcutaneously into immunodeficient mice and treated by intratumoral injections in order to compare the therapeutic benefit of

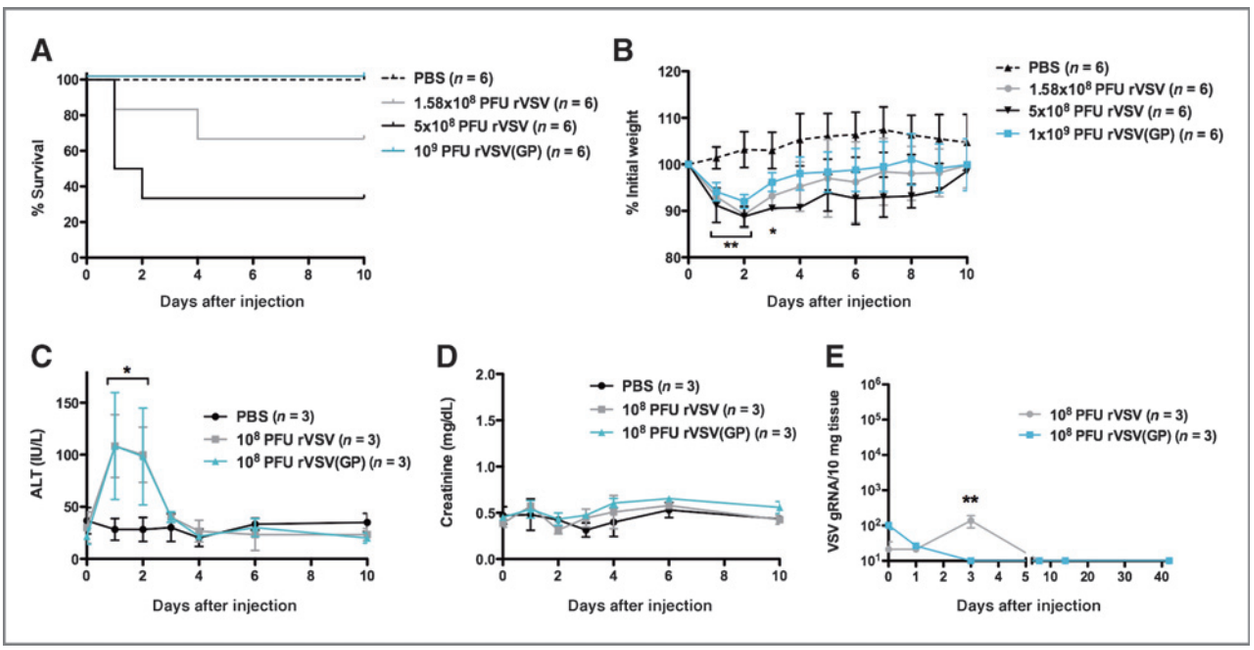

Figure 2. Systemic high-dose rVSV(GP) application is well tolerated. A and B, CD-1 mice ($n = 6$/cohort) were injected intravenously with escalating doses of up to 10^9 PFU rVSV(GP) and rVSV or PBS as controls. Animals were monitored for event-free survival (A) and for weight changes (B). Mean weight ± SDs of each cohort at the respective time-point is plotted. C and D, CD-1 mice ($n = 3$/cohort) were injected with a sublethal dose of 10^8 PFU rVSV(GP), rVSV, or PBS as controls. Blood samples were collected at the indicated time-points postinjection and serum was prepared. ALT (C) as well as creatinine levels (D) were determined as mean ± SD. E, CD-1 mice ($n = 3$/cohort and time-point) were injected intravenously with either 10^8 rVSV(GP), rVSV, or PBS. At each indicated time-point, $n = 3$ animals/cohort were sacrificed. RNA was purified from brain tissue. VSV genomic RNA (gRNA) levels were determined by reverse transcription real-time PCR and referenced against tissue weight. gRNA kinetics are shown with individual data points representing mean ± SD; *, $P < 0.05$; **, $P < 0.01$.

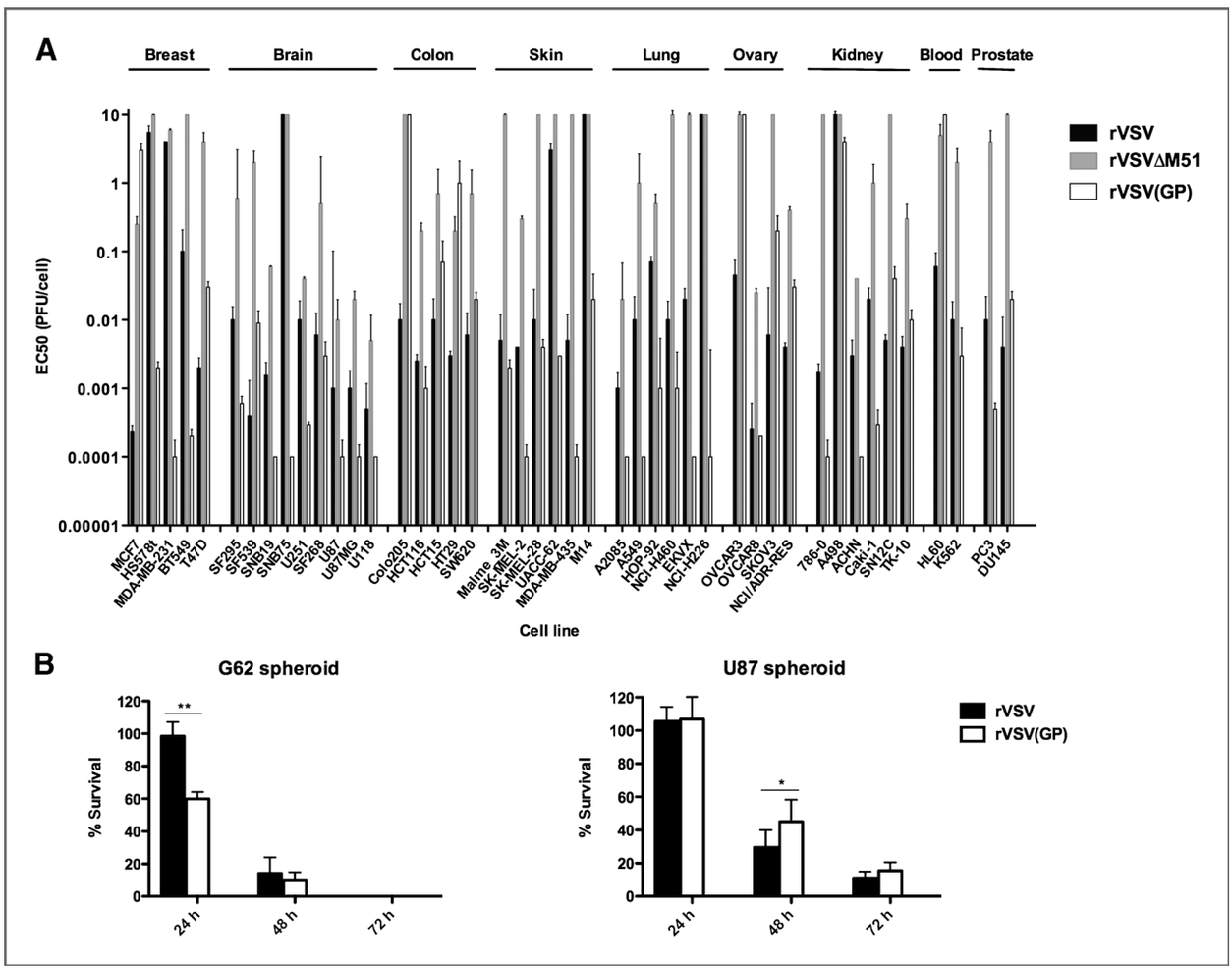

Figure 3. rVSV(GP) induces oncolysis in a broad spectrum of cancer cell types *in vitro*. A, the NCI60 human tumor cell lines were infected with an MOI of 0.00001 up to 10 (logarithmic steps) of rVSVΔM51, rVSV, and rVSV(GP) using a minimum of $n = 4$ technical replicates. ED_{50} values (PFU/cell) were determined as the respective MOIs were 50% survival was observed at 72 hours postinfection compared with untreated controls. B, G62 and U87 human glioblastoma cells were grown as multicellular tumor spheroids on agar and were infected with rVSV(GP) or rVSV at an MOI of 0.1. Cell viability was assayed at the indicated time-points postinfection via WST-1 assay compared with untreated controls. Bars represent mean ± SD of $n = 3$ independent experiments performed in dodecaplicates; *, $P < 0.05$; **, $P < 0.01$.

rVSV-GFP and rVSV(GP)-GFP. Both viruses were effective in rapidly and consistently eliminating G62 subcutaneous tumors (Fig. 4A). Plaque assays from tumor lysates were performed 3 days postinfection and show productive infection and massive viral burst for rVSV-GFP and rVSV(GP)-GFP (Supplementary Fig. S6). However, long-term survival of treated animals was strikingly different. Animals receiving therapeutic doses of rVSV(GP)-GFP were durably cured (Fig. 4B). However, although rVSV-GFP was also effective at eliminating the tumors, 90% of mice developed severe neurologic symptoms (hind limb paralysis, ataxia) shortly before tumors had regressed completely and ultimately succumbed to neurologic disease (Fig. 4B and C). Observed symptoms were typical for VSV-induced encephalitis as described previously (33). Indeed, replication of rVSV-GFP within the brain could be detected by immunohistochemistry (a representative slice is shown in Fig. 4C) and by quantitative RT-PCR (data not shown). Hence, although rVSV-GFP was administered intratumorally at a relatively low dose (2×10^5 PFU), its amplification within the tumor and eventual spread to the CNS led to death in the majority of animals. In contrast, no virus was detected by PCR or immunohistochemistry in the brains of rVSV(GP)-GFP–treated animals (data not shown). Thus, even in immunocompromised mice, rVSV(GP)-GFP was an effective oncolytic agent, rapidly replicating in the tumor (Fig. 4D and Supplementary Fig. S6) without causing neurotoxicity.

We next tested the antitumoral efficacy of rVSV(GP)-GFP in several orthotopic brain cancer models. rVSV-GFP treatment groups were omitted as an intracranial replication of rVSV induces fatal encephalitis within a few days (Fig. 1). First, rVSV (GP)-GFP was administered systemically to treat orthotopic U87 gliomas as it is known that this tumor locally disrupts the blood–brain barrier (8). Injection of 10^8 PFU rVSV(GP)-GFP i.v. led to an effective infection of gliomas with widespread virus

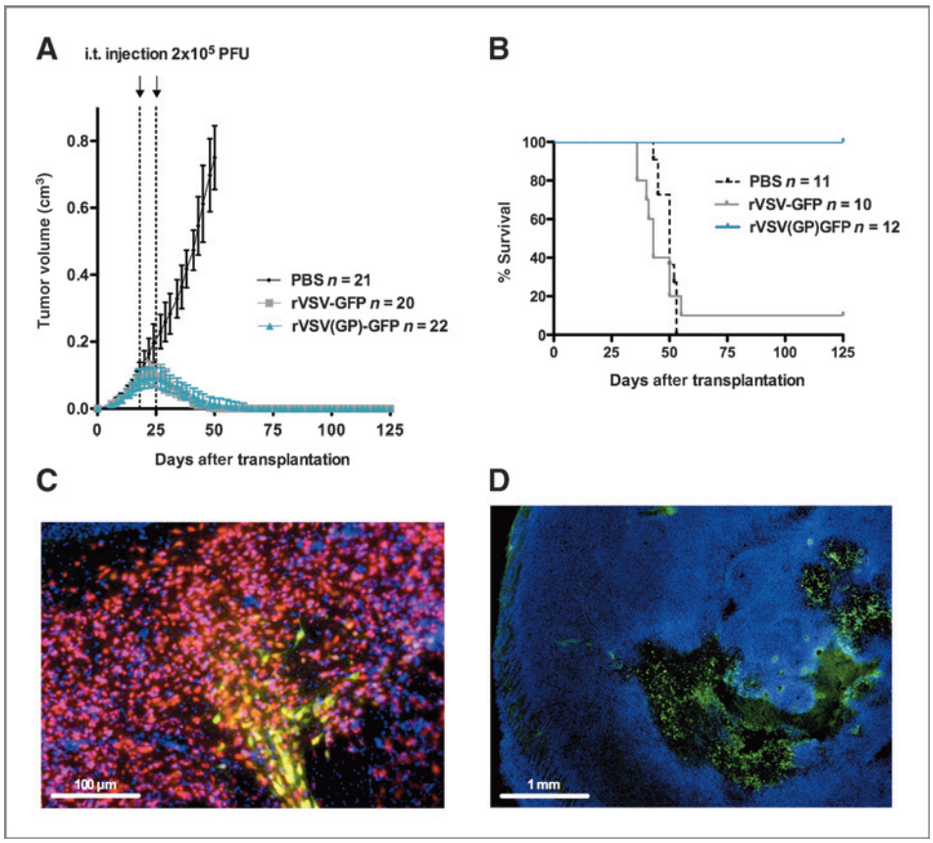

Figure 4. Intratumoral rVSV(GP) administration in subcutaneous G62 human glioblastoma xenografts leads to tumor clearance and event-free survival. 2×10^5 PFU/dose rVSV(GP)-GFP, rVSV-GFP, or PBS was injected intratumorally into subcutaneous bilateral G62 human glioblastoma xenografts in NOD/SCID mice at days 18 and 25 posttransplantation (dpt). Animals were monitored for tumor growth (A) as well as for event-free survival (B) for more than a period of 125 dpt. C, immunohistochemical analysis of coronal brain stem sections (dorsal raphe nucleus) from rVSV-GFP–treated mice after development of neuropathogenesis. Neurons were stained with mouse anti-NeuN (clone A60) primary and Alexa Fluor 568–conjugated secondary antibody (red). Replicating rVSV-GFP is shown in green. Nuclear counterstaining was performed with TO-PRO-3 iodide (blue). D, immunohistochemical analysis of rVSV(GP)-GFP dissemination within subcutaneous tumors at 3 days postinfection. Nuclear counterstaining was performed with TO-PRO-3 iodide (blue).

distribution, cellular disintegration, and blebbing as typical signs of virally mediated oncolysis (Fig. 5A). Strikingly, despite the massive infection and virus replication within the RFP-expressing tumor bulk, rVSV(GP)-GFP did not spread into normal brain tissue surrounding the tumor. In PBS-injected control animals, severe neurologic symptoms associated with uncontrolled tumor growth occurred, translating to a median survival for these mice of 33 days posttumor transplantation (dpt; Fig. 5B). In contrast, rVSV(GP)-GFP treatment considerably increased the lifespan of mice, leading to either ≈2-fold prolonged survival (up to 71 dpt) or long-term event-free survival (up to >125 dpt). Both the single- and multidose rVSV(GP)-GFP–treated cohorts had significant tumor-free survival (6/9 and 8/9 long-term survivors, respectively) and the necropsy of symptomatic animals revealed that tumor regrowth and not virus replication was the cause of neurologic symptoms. When animals suffered tumor relapse, samples of recurring tumors were cultured *in vitro* and found to still be susceptible to virus infection and killing (Supplementary Fig. S7). Thus, relapse was most likely a result of insufficient virus spread or some innate antiviral activity of NK cells as opposed to tumors evolving to a resistant phenotype.

In parallel, we also tested the therapeutic efficacy of intracranially administered rVSV(GP)-GFP in a syngeneic CT2A glioma model. A single injection of rVSV(GP)-GFP into established CT2A tumors implanted in the brains of C57Bl/6 mice led to a significantly prolonged median survival compared with PBS-treated controls (81 dpt vs. 29 dpt; $P = 0.0018$) and 5 of 10 animals even showed long-term event-free survival (Fig. 5C).

Besides malignant gliomas, secondary brain cancers that arise as result of metastasis from extracranial tumors are also an important clinical consideration. Accordingly, we tested the ability of rVSV(GP)-GFP to impact the growth of murine colon tumors (CT26) implanted in the brains of Balb/C mice. A single injection of rVSV(GP)-GFP intratumorally resulted in 9/11-treated mice having long-term durable cures with no signs of off-target infections leading to neurotoxicity (Fig. 5D).

rVSV(GP) escapes humoral immunity and can be used in multidosing regimens

VSV is well known to trigger a rapid and robust nAb response in mice that is expected to hamper oncolytic efficacy upon repeated systemic application. The target of the nAb response is the extremely immunogenic VSV-G whereas LCMV-GP is believed to not induce a nAb response (34). Hence, we tested whether mice could mount a nAb response against rVSV(GP) when administered intravenously at the high doses required to be an effective oncolytic. Following a single intravenous dose of rVSVΔM51, a nAb response begins at day 3 postinfusion, peaks at day 7, and remains high for several weeks. However, rVSV(GP) intravenously does not elicit a detectable nAb response (Fig. 6D).

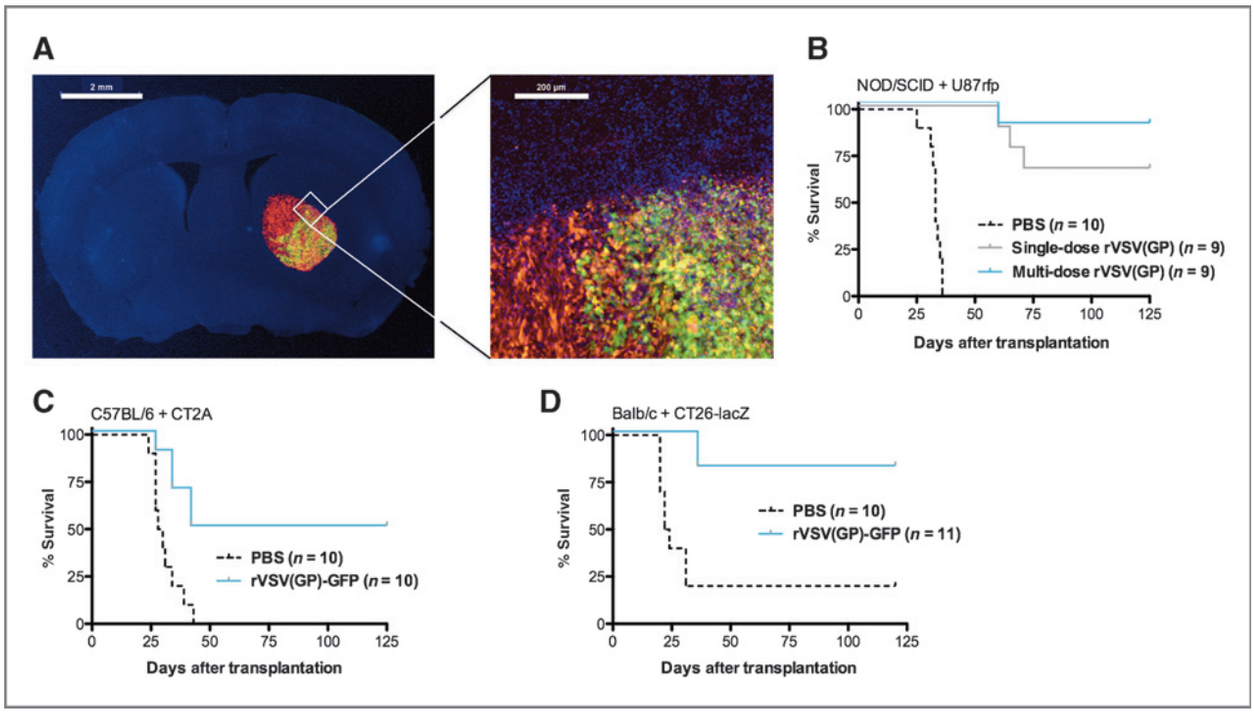

Figure 5. rVSV(GP) treatment led to long-term survival of both xenogeneic and syngeneic CNS tumor-bearing mice. A, $N = 3$ U87-RFP orthotopic glioma-bearing NOD/SCID mice were treated intravenously with a single dose of 10^8 PFU rVSV(GP)-GFP at 10 days posttransplantation (dpt). Animals were sacrificed at 3 days postinjection and immunohistochemical analysis of coronal brain sections was performed with TO-PRO-3 iodide as nuclear counterstain (blue). A representative fluorescent micrograph is shown with an arrow indicating the area of progressing cellular disintegration. B, cohorts of $n \geq 9$ U87-RFP orthotopic glioma-bearing NOD/SCID mice were treated intravenously with either single or multiple doses of 10^8 PFU rVSV(GP)-GFP at 10 dpt or 10, 17, and 24 dpt, respectively. Control mice were injected with PBS. Animals were monitored for event-free survival more than a period of 125 dpt. C, CT2A orthotopic glioma-bearing C57Bl/6 mice ($n = 10$/cohort) were treated intracranially with either PBS or 10^8 PFU rVSV(GP)-GFP at 7 dpt. Mice were monitored for event-free survival for more than a period of 120 days. D, CT26-lacZ syngeneic colon carcinoma brain metastases-bearing Balb/c mice ($n \geq 10$/cohort) were treated intracranially with either PBS or 2.5×10^7 PFU rVSV(GP)-GFP at 7 dpt. Mice were monitored for event-free survival for more than a period of 120 dpt.

To help determine the impact of rVSV(GP) escaping the nAb response, rVSVΔM51- and rVSV(GP)-preimmunized Balb/c mice were engrafted with subcutaneous CT26 tumors and subsequently treated intratumorally or intravenously with the respective virus (Fig. 6B). At 48 hours posttreatment, mice were sacrificed and tumors were analyzed for viral load via quantitative RT-PCR. As could be predicted by the nAb titration (Fig. 6A), rVSV(GP) was able to reach the tumor with VSV gRNA being detectable in all preimmunized animals. In striking contrast, in all mice that were preimmunized with rVSVΔM51 and subsequently infected with the same virus no virus genomes could be detected. All tumor tissues collected from non-preimmunized control animals were positive for VSV gRNA (Fig. 6B).

In addition to adaptive humoral immunity, VSV can also be inactivated to some extent in naïve human serum (NHS) because of complement activation. Earlier Welsh and colleagues (35) reported that LCMV (Armstrong strain) generally resists inactivation by human complement and thus we tested rVSV and rVSV(GP) for stability in NHS with and without complement. As expected, NHS is able to reduce rVSV titers more than 100-fold, an activity that is lost after heat inactivation of complement. In contrast, rVSV(GP) is insensitive to human complement (Fig. 6C) and remains stable over the length of the experiment.

Discussion

The challenge in creating an effective OV is to establish a balance between safety and potency to eventually achieve clinical benefit. VSV exhibits many of the attributes that are desirable in an oncolytic therapeutic (reviewed in ref. 13). However, widespread regulatory approval and clinical implementation of nonattenuated strains is unlikely because of the virus' inherent neurotoxicity. Recently, a first clinical trial to evaluate the safety of an interferon β (IFNβ)-expressing VSV after intratumoral delivery into liver cancer was started (www.clinicaltrials.gov; NCT01628640). Similar to attenuated VSV recombinants, which are engineered to have an impaired ability to antagonize cellular antiviral responses, the IFNβ transgene of the study virus restricts viral spread to IFN-unresponsive tumor cells (9–11, 21, 36). However, the extent of defective IFN responses in malignancies is variable and thus such vectors may require alternative strategies to improve their efficacy (37–39).

The approach described here allowed us to use an optimal OV but eliminate neurotoxicity. Remarkably, the replacement of VSV-G with LCMV-GP allowed us to convert a virus (rVSV)

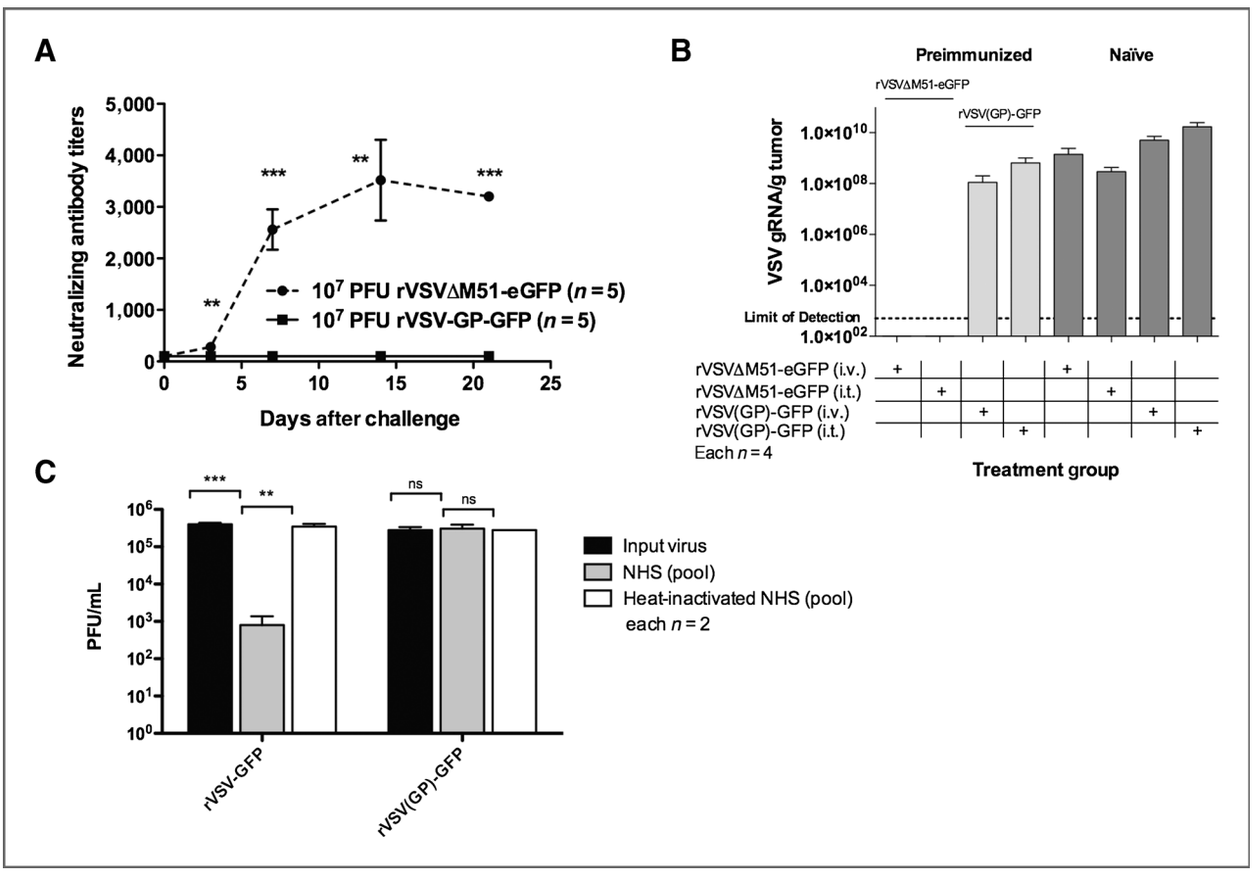

Figure 6. rVSV(GP) escapes innate and adaptive humoral immunity. A, Balb/c mice were infected intravenously with 10^7 PFU rVSV(GP)-GFP or rVSVΔM51 ($n = 5$/cohort). Serum samples were collected at the indicated time-points and tested in neutralization assays for nAb titers against the respective virus. Relative nAb titers were determined as mean ± SD from the dilution at which 50% cytopathic effect was observed on BHK-21 cells. B, Balb/c mice were immunized with a single 10^7 PFU dose intravenously of either rVSVΔM51-eGFP or rVSV(GP)-GFP. At 10 days postimmunization, preimmunized and naïve animals were subcutaneously grafted with 3×10^5 CT26 cells. Palpable tumors were treated with 10^8 PFU intravenously or 10^7 PFU intratumorally of either rVSVΔM51-eGFP or rVSV(GP)-GFP. At 48 hours posttreatment, animals were sacrificed and tumors were removed. Tumor viral load was determined as VSV genomic RNA (gRNA) via quantitative RT-PCR. Results for preimmunized animals are shown as light gray bars, for naïve animals as dark gray bars. Bars represent mean ± SEM from $n = 4$ tumors per cohort. C, 10^5 PFU/mL rVSV and rVSV(GP) were preincubated in duplicates ($n = 2$) with NHS, heat-inactivated NHS, or DMEM/10% FBS as input virus control. Preincubated samples were titrated on BHK-21 cells via plaque assay. Titers represent means ± SD; **, $P < 0.01$; ***, $P < 0.001$.

that is lethal when injected intracranially at any dose, to a benign agent that can be safely administered at doses in excess of 10^8 PFU (Fig. 1). Indeed, this chimeric virus has a much improved intracranially safety profile over rVSVΔM51, an oncolytic virus candidate with an impaired anti-IFN response (11). In addition, because rVSV(GP) harbors an intact matrix (M) protein that can attenuate cellular IFN responses, it has dramatically increased potency on a number of tumor cell lines compared with rVSVΔM51 (Fig. 3A). Brain cancer cell lines seem particularly susceptible to rVSV(GP)-mediated oncolysis. Importantly, in a previous study we showed that in addition to glioma cell lines, primary human glioma–derived stem cells (hGSC) were equally susceptible to LCMV-pseudotyped VSV vectors (20).

The exquisite tumor specificity of rVSV(GP) was best illustrated in an orthotopic brain cancer model (Fig. 5A and B) where robust virus replication was restricted to tumor cells only. Here, rVSV(GP)'s main mode of action is active replication and spread throughout the tumor, thereby lysing all malignant cells. The "snap shots" of rVSV(GP) gene expression in Fig. 5A as well as in Fig. 4D show that the virus has only partially penetrated the tumor at a relatively early time-point posttreatment while eventually all cancer cells were eliminated as seen by necropsy at the end of the experiment. In the immunodeficient mouse models, no specific antiviral immunity can be induced that could restrict rVSV(GP) replication. However, no specific anticancer immunity is induced that could help eliminate residual cancer cells. The xenogenic reactivity of NK cells in NOD/SCID mice, which is not able to control growth of the U87-tumor formation, could still have contributed to elimination of cancer cells in the xenotransplant models. In addition, in the immunocompetent mouse models, an antitumor immune response may well have contributed to the therapeutic effect. These issues are currently under investigation. Nonetheless, in summary, considering both safety and efficacy data, rVSV(GP) exhibits

a tremendously increased therapeutic window compared with rVSV in brain cancer tumor models.

The beneficial tropism of chimeric rVSV(GP) directly correlates with the respective envelope glycoprotein. The VSV glycoprotein is a critical determinant of the neurotoxicity of VSV and is known to mediate the infection of a wide variety of eukaryotic cell types. This pantropism is because of the widespread expression of the LDL receptor, which serves as the major cellular entry port of wtVSV (40). In contrast, previous reports provide evidence that the LCMV glycoprotein used in our studies binds with exceptionally high affinity to α-dystroglycan (αDG), a cell surface protein that is found on many types of normal brain cells (41, 42). However, it is known that the ability of αDG to function as a virus receptor is dependent upon posttranslational modifications and thus the inability of rVSV(GP) to infect normal neurons could be related to differential glycosylation patterns or the extent of αDG expression on the cell surface (43, 44). Alternatively, an unknown critical coreceptor for GP may be missing from neurons, a mechanism of infection restriction seen in other OVs (45). This hypothesis is underscored by findings of Calogero and colleagues (46) in combination with our own obtained results. Calogero and colleagues demonstrated that αDG expression was strongly reduced in human glioblastoma (e.g., biopsies and cell lines like U87-MG), which, however, proved an exceptionally good target for rVSV(GP)-based virotherapy (Figs. 3 and 5). Because the underlying molecular explanation of the beneficial tropism as well as the precise IFN-inducing capacity of rVSV(GP) remains largely elusive, these are ongoing areas of research.

Recently, two clinical studies have demonstrated that certain OVs can be delivered to tumor beds despite the presence of some level of circulating antibody (47, 48). Nevertheless, it is widely believed that nAbs that arise during therapy will significantly abrogate therapeutic efficacy of repeated systemic OV applications (13, 49). Remarkably, even when administered intravenously at therapeutic doses, rVSV(GP) did not elicit detectable nAb titers (Fig. 6A). This is consistent with earlier findings by Pinschewer and colleagues as well as Planz and colleagues. Although VSV rapidly induces nAbs against VSV-G, nAbs directed against LCMV-GP are, if at all, induced only in chronically infected mice after more than 50 days (34, 50). Hence, although we could not observe nAbs in our experiments, long-term repeated applications may possibly lead to low-titer nAb response as described for chronic LCMV infections. However, here, the observed escape from humoral adaptive immunity even allows for efficient systemic delivery of rVSV(GP) to subcutaneous tumors in preimmunized mice, whereas nAbs induced by rVSVΔM51 preimmunization completely block rVSVΔM51 delivery (Fig. 6B). Even in the absence of nAbs VSV can be at least partially inactivated by human complement, whereas rVSV(GP) is completely resistant to complement inactivation (Fig. 6C). Taken together, escape from humoral immune responses is expected to allow an effective long-term, systemic multidosing rVSV(GP) regimen in the clinical setting, an attribute that may well be unique among OV platforms. In this regard, an extensive study is currently ongoing in which we are analyzing the effectiveness of rVSV versus rVSV(GP) upon repeated applications in syngeneic tumor models. As the humoral immune escape properties are mediated by the envelope glycoprotein, LCMV-GP pseudotyping might be a comprehensive strategy to circumvent nAb induction that is also feasible for other enveloped OVs and vectored vaccines.

Obviously, as rVSV(GP) is a hybrid virus that does not occur naturally, preclinical safety assessments must be extensive and thorough. As with all replicative OVs, shedding of the virus via bodily fluids into the environment and potential for subsequent transmission must be absolutely excluded before it can be used in the clinic. However, if preclinical analyses prove this chimeric virus to be safe, the lack of neurotoxicity, potent tumor killing activity, and increased stability in nonimmune and immune serum strongly support the advancement of rVSV(GP) as a clinical oncolytic virus candidate especially for malignancies with dismal prognosis such as glioblastoma.

Disclosure of Potential Conflicts of Interest

D. von Laer has ownership interest (including patents) from PCT/EP09/07230: LCMV-GP-VSV pseudotyped vectors and tumor-infiltrating virus producing cells for the therapy of tumors (US2011/0250188; DE 10 2008 050 860.8, Priority: 08.10.2008). No potential conflicts of interest were disclosed by the other authors.

Authors' Contributions

Conception and design: A. Muik, L.J. Stubbert, J.C. Bell, D. von Laer
Development of methodology: A. Muik, L.J. Stubbert, R.Z. Jahedi, R. Tober, B. Yadollahi
Acquisition of data (provided animals, acquired and managed patients, provided facilities, etc.): A. Muik, L.J. Stubbert, Y. Geiβ, J. Kimpel, C. Dold, A. Volk, S. Klein, U. Dietrich, B. Yadollahi, T. Falls, H. Miletic, D. Stojdl, J.C. Bell
Analysis and interpretation of data (e.g., statistical analysis, biostatistics, computational analysis): A. Muik, L.J. Stubbert, R.Z. Jahedi, J. Kimpel, S. Klein, B. Yadollahi, H. Miletic, J.C. Bell
Writing, review, and/or revision of the manuscript: A. Muik, L.J. Stubbert, J.C. Bell, D. von Laer
Administrative, technical, or material support (i.e., reporting or organizing data, constructing databases): L.J. Stubbert, R.Z. Jahedi, Y. Geiβ, U. Dietrich, B. Yadollahi
Study supervision: D. Stojdl, D. von Laer

Grant Support

This work was supported by grants from the Wilhelm-Sander-Foundation, the Deutsche Forschungsgemeinschaft, the Hertie Foundation, the FWF Austrian Science Fund (P25499-B-13), the LOEWE Center for Cell and Gene Therapy Frankfurt, and the Schering Foundation.

The costs of publication of this article were defrayed in part by the payment of page charges. This article must therefore be hereby marked *advertisement* in accordance with 18 U.S.C. Section 1734 solely to indicate this fact.

Received November 18, 2013; revised March 28, 2014; accepted April 6, 2014; published OnlineFirst May 8, 2014.

References

1. Ohgaki H. Epidemiology of brain tumors. Methods Mol Biol 2009;472:323–42.
2. Wen PY, Kesari S. Malignant gliomas in adults. N Engl J Med 2008;359:492–507.
3. Zemp FJ, Corredor JC, Lun X, Muruve DA, Forsyth PA. Oncolytic viruses as experimental treatments for malignant gliomas: using a scourge to treat a devil. Cytokine Growth Factor Rev 2010;21:103–17.

4. Russell SJ, Peng KW, Bell JC. Oncolytic virotherapy. Nat Biotech 2012;30:658–70.
5. Ahmed M, Cramer SD, Lyles DS. Sensitivity of prostate tumors to wild type and M protein mutant vesicular stomatitis viruses. Virology 2004;330:34–49.
6. Capo-chichi CD, Yeasky TM, Heiber JF, Wang Y, Barber GN, Xu XX. Explicit targeting of transformed cells by VSV in ovarian epithelial tumor-bearing Wv mouse models. Gynecol Oncol 2010;116: 269–75.
7. Ebert O, Shinozaki K, Huang TG, Savontaus MJ, Garcia-Sastre A, Woo SL. Oncolytic vesicular stomatitis virus for treatment of orthotopic hepatocellular carcinoma in immune-competent rats. Cancer Res 2003;63:3605–11.
8. Ozduman K, Wollmann G, Piepmeier JM, van den Pol AN. Systemic vesicular stomatitis virus selectively destroys multifocal glioma and metastatic carcinoma in brain. J Neurosci 2008;28: 1882–93.
9. Stojdl DF, Lichty B, Knowles S, Marius R, Atkins H, Sonenberg N, et al. Exploiting tumor-specific defects in the interferon pathway with a previously unknown oncolytic virus. Nat Med 2000;6: 821–5.
10. Hadaschik BA, Zhang K, So AI, Fazli L, Jia W, Bell JC, et al. Oncolytic vesicular stomatitis viruses are potent agents for intravesical treatment of high-risk bladder cancer. Cancer Res 2008;68:4506–10.
11. Stojdl DF, Lichty BD, tenOever BR, Paterson JM, Power AT, Knowles S, et al. VSV strains with defects in their ability to shutdown innate immunity are potent systemic anti-cancer agents. Cancer Cell 2003; 4:263–75.
12. Lyles DS, Rupprecht CE. Fields virology. 5th ed. Lippincott Williams & Wilkins; 2006. p. 1364–94.
13. Hastie E, Grdzelishvili VZ. Vesicular stomatitis virus as a flexible platform for oncolytic virotherapy against cancer. J Gen Virol 2012;93: 2529–45.
14. van den Pol AN, Dalton KP, Rose JK. Relative neurotropism of a recombinant rhabdovirus expressing a green fluorescent envelope glycoprotein. J Virol 2002;76:1309–27.
15. Johnson JE, Nasar F, Coleman JW, Price RE, Javadian A, Draper K, et al. Neurovirulence properties of recombinant vesicular stomatitis virus vectors in non-human primates. Virology 2007;360: 36–49.
16. Quiroz E, Moreno N, Peralta PH, Tesh RB. A human case of encephalitis associated with vesicular stomatitis virus (Indiana serotype) infection. Am J Trop Med Hyg 1988;39:312–4.
17. Kelly EJ, Nace R, Barber GN, Russell SJ. Attenuation of vesicular stomatitis virus encephalitis through microRNA targeting. J Virol 2010;84:1550–62.
18. Edge RE, Falls TJ, Brown CW, Lichty BD, Atkins H, Bell JC. A let-7 microRNA-sensitive vesicular stomatitis virus demonstrates tumor-specific replication. Mol Ther 2008;16:1437–43.
19. Ayala-Breton C, Barber GN, Russell SJ, Peng KW. Retargeting vesicular stomatitis virus using measles virus envelope glycoproteins. Hum Gene Ther 2012;23:484–91.
20. Muik A, Kneiske I, Werbizki M, Wilflingseder D, Giroglou T, Ebert O, et al. Pseudotyping vesicular stomatitis virus with lymphocytic choriomeningitis virus glycoproteins enhances infectivity for glioma cells and minimizes neurotropism. J Virol 2011;85: 5679–84.
21. Clarke DK, Nasar F, Lee M, Johnson JE, Wright K, Calderon P, et al. Synergistic attenuation of vesicular stomatitis virus by combination of specific G gene truncations and N gene translocations. J Virol 2007;81:2056–64.
22. Cooper D, Wright KJ, Calderon PC, Guo M, Nasar F, Johnson JE, et al. Attenuation of recombinant vesicular stomatitis virus-human immunodeficiency virus type 1 vaccine vectors by gene translocations and g gene truncation reduces neurovirulence and enhances immunogenicity in mice. J Virol 2008;82:207–19.
23. Beyer WR, Westphal M, Ostertag W, von Laer D. Oncoretrovirus and lentivirus vectors pseudotyped with lymphocytic choriomeningitis virus glycoprotein: generation, concentration, and broad host range. J Virol 2002;76:1488–95.
24. Miletic H, Fischer YH, Giroglou T, Rueger MA, Winkeler A, Li H, et al. Normal brain cells contribute to the bystander effect in suicide gene therapy of malignant glioma. Clin Cancer Res 2007;13: 6761–8.
25. Miletic H, Fischer YH, Neumann H, Hans V, Stenzel W, Giroglou T, et al. Selective transduction of malignant glioma by lentiviral vectors pseudotyped with lymphocytic choriomeningitis virus glycoproteins. Hum Gene Ther 2004;15:1091–100.
26. Beyer WR, Miletic H, Ostertag W, von Laer D. Recombinant expression of lymphocytic choriomeningitis virus strain WE glycoproteins: a single amino acid makes the difference. J Virol 2001;75:1061–4.
27. Seyfried TN, El-Abbadi M, Roy ML. Ganglioside distribution in murine neural tumors. Mol Chem Neuropathol 1991;17:147–67.
28. Boritz E, Gerlach J, Johnson JE, Rose JK. Replication-competent rhabdoviruses with human immunodeficiency virus type 1 coats and green fluorescent protein: entry by a pH-independent pathway. J Virol 1999;73:6937–45.
29. Muik A, Dold C, Geiss Y, Volk A, Werbizki M, Dietrich U, et al. Semireplication-competent vesicular stomatitis virus as a novel platform for oncolytic virotherapy. J Mol Med (Berl) 2012.
30. Diallo JS, Vähä-Koskela M, Le Boeuf F, Bell J. Propagation, purification, and *in vivo* testing of oncolytic vesicular stomatitis virus strains. Methods Mol Biol 2012;797:127–40.
31. Welsh RM, O'Donnell CL, Reed DJ, Rother RP. Evaluation of the Galα1-3Gal epitope as a host modification factor eliciting natural humoral immunity to enveloped viruses. J Virol 1998;72:4650–6.
32. Simon ID, van Rooijen N, Rose JK. Vesicular stomatitis virus genomic RNA persists *in vivo* in the absence of viral replication. J Virol 2010;84:3280–6.
33. Sur JH, Allende R, Doster AR. Vesicular stomatitis virus infection and neuropathogenesis in the murine model are associated with apoptosis. Vet Pathol 2003;40:512–20.
34. Pinschewer DD, Perez M, Jeetendra E, Bachi T, Horvath E, Hengartner H, et al. Kinetics of protective antibodies are determined by the viral surface antigen. J Clin Invest 2004;114:988–93.
35. Welsh RM. Host cell modification of lymphocytic choriomeningitis virus and Newcastle disease virus altering viral inactivation by human complement. J Immunol 1977;118:348–54.
36. Wollmann G, Rogulin V, Simon I, Rose JK, van den Pol AN. Some attenuated variants of vesicular stomatitis virus show enhanced oncolytic activity against human glioblastoma cells relative to normal brain cells. J Virol 2010;84:1563–73.
37. Blackham AU, Northrup SA, Willingham M, D'Agostino RB Jr., Lyles DS, Stewart JHt. Variation in susceptibility of human malignant melanomas to oncolytic vesicular stomatitis virus. Surgery 2013;153: 333–43.
38. Paglino JC, van den Pol AN. Vesicular stomatitis virus has extensive oncolytic activity against human sarcomas: rare resistance is overcome by blocking interferon pathways. J Virol 2011;85:9346–58.
39. Zhang KX, Matsui Y, Hadaschik BA, Lee C, Jia W, Bell JC, et al. Down-regulation of type I interferon receptor sensitizes bladder cancer cells to vesicular stomatitis virus-induced cell death. Int J Cancer 2009; 127:830–8.
40. Finkelshtein M, Werman A, Novick D, Barak S, Rubinstein M. LDL receptor and its family members serve as the cellular receptor for vesicular stomatitis virus. PNAS 2013;110:7306–11.
41. Smelt SC, Borrow P, Kunz S, Cao W, Tishon A, Lewicki H, et al. Differences in affinity of binding of lymphocytic choriomeningitis virus strains to the cellular receptor α-dystroglycan correlate with viral tropism and disease kinetics. J Virol 2001;75:448–57.
42. Zaccaria ML, Di Tommaso F, Brancaccio A, Paggi P, Petrucci TC. Dystroglycan distribution in adult mouse brain: a light and electron microscopy study. Neuroscience 2001;104:311–24.
43. Kunz S, Rojek JM, Kanagawa M, Spiropoulou CF, Barresi R, Campbell KP, et al. Posttranslational modification of α-dystroglycan, the cellular receptor for arenaviruses, by the glycosyltransferase LARGE is critical for virus binding. J Virol 2005;79:14282–96.
44. Satz JS, Ostendorf AP, Hou S, Turner A, Kusano H, Lee JC, et al. Distinct functions of glial and neuronal dystroglycan in the developing and adult mouse brain. J Neurosci 2010;30:14560–72.

45. Anderson BD, Nakamura T, Russell SJ, Peng KW. High CD46 receptor density determines preferential killing of tumor cells by oncolytic measles virus. Cancer Res 2004;64:4919–26.
46. Calogero A, Pavoni E, Gramaglia T, D'Amati G, Ragona G, Brancaccio A, et al. Altered expression of α-dystroglycan subunit in human gliomas. Cancer Biol Ther 2006;5:441–8.
47. Adair RA, Roulstone V, Scott KJ, Morgan R, Nuovo GJ, Fuller M, et al. Cell carriage, delivery, and selective replication of an oncolytic virus in tumor in patients. Sci Transl Med 2012;4:138ra77.
48. Pesonen S, Diaconu I, Kangasniemi L, Ranki T, Kanerva A, Pesonen SK, et al. Oncolytic immunotherapy of advanced solid tumors with a CD40L-expressing replicating adenovirus: assessment of safety and immunologic responses in patients. Cancer Res 2012;72:1621–31.
49. Kueberuwa G, Cawood R, Seymour LW. Blood compatibility of enveloped viruses. Curr Opin Mol Ther 2010;12:412–20.
50. Planz O, Seiler P, Hengartner H, Zinkernagel RM. Specific cytotoxic T cells eliminate B cells producing virus neutralizing antibodies. Nature 1996;382:726–29.